Ag Nanoparticles on Glycine Modified Graphene Oxide for Catalytic, Electrocatalytic and Antibacterial Applications

Soghra Fathalipour[1], Sima Pourbeyram*[1], Sanaz Lotfi[1], Rasul Bulgar[2]

1. Department of Chemistry, Payame Noor University, P.O. Box 19395-4697, Tehran, Iran
2. Faculty of Basic Science, Shahid Madani University, Azarbaijan, Iran

Abstract

Silver nanoparticles (Ag NPs)-reduced graphene oxide was prepared through the in situ nucleation of Ag NPs on reduced, modified GO (rMGO). Glycine was used as a green reducing as well as modifier agent for GO to obtain rMGO. Nucleation of Ag NPs on rMGO was carried out at 80 °C at aqueous media. UV-Vis, FT-IR, and XRD techniques confirmed the reduction, modification, and synthesis of Ag NPs. Meanwhile, the morphology of rMGO and rMGO-Ag nanocomposite was investigated with SEM and TEM images. The synthesized nanocomposite showed excellent catalytic behavior for the reduction of 4-nitrophenol (4-NP) by NaBH₄. The electrocatalytic behavior of Ag NPs on rMGO for electroreduction of H_2O_2 was investigated by cyclic voltammetry (CV). In the optimum condition, H_2O_2 was determined with a detection limit of 9.4 µM and sensitivity of 0.52 µAµM⁻¹. In addition, with the investigation of MIC data of nanocomposite, it was distinguished that this compound has excellent antibacterial activity.

1. INTRODUCTION

Recently, Ag metal nanoparticles (NPs) have been attractive because of unique physical, chemical properties [1] and potential applications in surface-enhanced Raman scattering (SERS) [2], catalysis [3], imaging [4], biomedical [1, 5], and antibacterial aspects [6]. Ag NPs due to the the high surface energy, aggregate and to solve this problem, templates or stabilizing molecules are used [7].

The controlled synthesis of Ag NPs on the surface of graphene (a 2-D nanomaterial) and its derivatives has attracted attention due to its unique physical and chemical properties [8-10] and applications in catalysis [11], Surface-Enhanced Raman scattering (SERS) [12], sensor and antibacterial applications [13]. Graphene-Ag nanocomposites have been synthesized by various methods [14] that some of these approaches have various disadvantages such as: use of toxic reducing agents (NaBH₄, hydrazine, and hydroquinone), and aggregation of graphene and Ag NPs because of π-π stacking interactions between graphene sheets and Ag NPs [15]. Among different methods, in situ green synthesis is more critical because of its simplicity and biocompatibility [11, 13]. Sugar [16], ascorbic acid [17], starch-based materials [18], and amino acids [17] have been used as environmentally friendly, reducing agents for GO. GO containing functional groups (OH, epoxy, and carboxyl group) can be dispersed in polar solvents like

water and hydrolyze to the carboxylic acid group [19]. So, modification of GO with various compounds such as polymers, organic crystals, and biomaterials is attractive for many scientists and can be a suitable template for Ag NPs [11]. These modifier groups allow Ag nanoparticles to interact with the GO sheets via electrostatic binding or charge-transfer interactions. Glycine, the essential amino acid, has been used as a reducing agent and modifier for GO [20] and noble metal NPs [21, 22]. So, the using of this compound in the preparation of Graphene-Ag nanocomposite without reducing agent can produce eco-friendly green nanocomposite with an appropriate application.

4-Nitrophenol (4-NP) is a byproduct of the production reaction of pesticides and synthetic dyes and has a strong corrosive effect on body tissue (nervous system, liver, and kidneys) [23]. This compound due to its high stability and solubility in aqueous media, pollute water and environmental. So, the removal of this toxic compound from the environmental and its converting to 4-aminophenol (4-AP) is essential. 4-AP is a valuable intermediate in the manufacturing of dyes, pharmaceuticals, and antioxidants. In comparison to different techniques of elimination [24], catalytic reduction of 4-NP to 4-AP by the sodium borohydride (NaBH₄) is one of the most appropriate methods [25]. Recently, noble metal NPs have been attractive as effective catalysts for the degradation

of different hazardous materials like dyes, phenol derivatives, *etc*. [11, 26]. The researchers have used Ag nanoparticles and graphene-Ag nanocomposites as a catalyst in the reduction of 4-NP [11, 27]. Das and coworkers showed synthesized Ag-reduced graphene oxide in the presence of L-Arginine have high activity catalytic for the 4-NP reduction [11]. Aditya *et al.* studied the reduction of nitro phenol to aminophenol with a reducing agent in an aqueous medium by a metal or metal oxide catalyst [28]. Wu et al. [29] used GO-Au–Ag nanocomposite in the reduction of 4-NP and displayed that owing to GO, NPs show high catalytic efficiency. In environmental for the removing of contaminants, graphene-silver nanocatalysts must be biocompatable. Therefore, the green method should be used for the preparation of these nanocomposites.

In this work, an eco-friendly approach was selected for the preparation of reduced modified GO-Ag based on glycine. Then the catalytic activity in the reduction of 4-NP , electrocatalytic activity toward H_2O_2 determination, and antibacterial activity against Escherichia coli (E. coli) and S-arouses was studied.

2. EXPERIMENTAL
2.1. Materials
Silver nitrate (AgNO3), graphite, glycine (Gly), sodium hydroxide (NaOH), Sodium borohydride (NaBH4), 4-nitrophenol (4-NP), 4-nitroaniline (4-NA), ethanol (EtOH), hydrogen peroxide (H2O2), and acetone were purchased from Merck. All compounds used in this experiment were of analytical grade. Deionized (DI) water was used during the preparation of samples.

2.2. Synthesis of reduced modified GO–Ag (rMGO-Ag) nanocomposite
Graphite oxide (GO) was prepared by the oxidation of graphite powder according to the improved Hummers method [30]. For the modification of GO, GO (200 mg) was dispersed in DI water (20 ml), and then the solution of Gly (600 mg) and NaOH (320 mg) in DI water (20 ml) was added to the dispersed GO. The mixture was stirred for 24 h at room temperature and then centrifuged. Ethanol (10 ml) was poured into the colloidal dispersion, and the obtained precipitate was washed well with a mixture of H_2O/EtOH (1:1) and acetone, and finally dried in vacuum at 50 °C to obtain reduced modified GO (rMGO). After the modification of GO with Gly, AgNPs decorated rMGO was prepared by the best combination of rMGO and AgNO3.
In brief, rMGO powder (3.75mg) was dispersed

in water (5 ml) by sonication for one hour (h) to form exfoliated stable suspension. Then pH was adjusted at 12 with the solution of NaOH (1M). After that, the aqueous solution of $AgNO_3$ (50 mL, 0.24 mM) was poured into the suspension solution and mixed under ultrasonic for one h. Finally, the mixture was stirred in an oil bath at 80 °C for 16 hours, and then centrifuged to remove unreacted reagents. Finally, for the characterization and improving colloidal stability of nanocomposite, the resultant suspension was freeze-dried.

2.3. The catalytic behavior of synthesized nanocomposite
To investigate the catalytic activity of synthesized nanocomposite, rMGO-Ag nanocomposite (0.1 mg) was poured into an aqueous solution of nitro aromatic compound (1 ml, 0.5 mM). Then, the freshly prepared aqueous solution of $NaBH_4$ (1 ml, 0.08 M) was poured into the mixture and stirred at room temperature. The reduction of the nitro compound was studied by UV-Vis absorption. Finally, the catalyst was separated from the reaction mixture by column chromatography (ethyl acetate as a solvent). The nanocomposite was adsorbed on silica gel surface, separated, repeatedly washed with ethyl acetate, evaporate, and dried at a vacuum for the next cycle to study the reusability of the catalyst.

2.4. Antibacterial activity of nanocomposite
The antibacterial behavior of the rMGO-Ag nanocomposite against E-coli bacteria (ATCC 25922) and S-arouses (ATCC 29213) was studied by the Broth-dilution method. In brief, microbial suspensions equaling 0.5 McFarland ($1.5×106$ CFU) were prepared. As-synthesized rMGO-Ag colloidal solutions with different dilutions in nutrient broth (512, 256, 128, 64, 32, 16, 8 µg/ml) (2 ml) was poured into microbial suspensions (10 µl), and the tubes were incubated for 24 hours at 37°C. Müller-Hinton agar plates were cultured with 5µl of each tube and were incubated for another 24 h to determine the MIC.

2.5. Electrochemistry
Pencil lead with a diameter of 0.5 mm was inserted into a Teflon tube, so only 1 cm of its tip and end was exposed. By soldering a copper wire to the end exposed side of the PGE, electrical contact was made. PGE was immersed into the electrochemical cell containing a suspension of rMGO-Ag nanocomposite (0.1 mg) and the potential of the electrode was 12 cycles scanned at 50 mV s^{-1} in the range 1.2 to -1.0 V. The modified electrode then rinsed and transferred to

the uninfected cell containing HCl 0.1 M and the electrode potential was scanned until the stable response was achieved.

2.6. Instruments

Potentiostat/Galvanostat Autolab30 was used for electrochemical measurements on a conventional three-electrode glass cell containing a Pt rode as auxiliary, Ag/AgCl (3M KCl) as a reference and pencil graphite as working electrodes. Fourier Transform Infrared (FT-IR) spectra were studied with samples on KBr pellets over a frequency range of 4000–400 cm^{-1} in a Shimadzu 8400 spectrophotometer. X-ray diffraction (XRD) data were recorded by X Pert PRO made by Bruker-D8 ADVANCE 3000 X-Ray diffractometer with a Cu Kα radiation source (λ = 1.5406 Å). UV-Vis spectra of samples were studied by a UV-Vis spectrometer (PG Instruments T80) in the range between 200 nm and 500 nm. The morphology was investigated by the scanning electron microscope (SEM, CamScan-MV2300) and Transmission electron microscopy (TEM, PHILIPS CM30). Energy-dispersive X-ray spectroscopy (EDX) was done by an EDX detector on a scanning electron microscopy. Zeta potential was studied using a Zetasizer (ZEN3600, Malvern Instruments, UK).

3. RESULT AND DISCUSSION

The reaction route for the synthesis of rMGO-Ag nanocomposite was summarized in scheme.1.
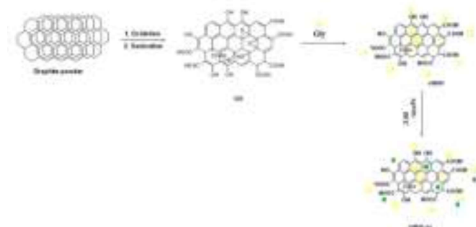
Scheme 1. Schematic diagram of the preparation of the rMGO-Ag nanocomposite.

3.1. Characterization of rMGO and rMGO-Ag nanocomposite

The structural changes during the modification are reflected in the UV-Vis absorption spectra (Fig. 1A). In UV-Vis of GO, the absorption peak at 228 nm corresponds to π-π* transitions of aromatic C=C bonds and a shoulder around 300 nm relates to n-π* transitions of C-O bonds [21]. After the modification of GO with Gly, the absorption peak of π-π* of GO shifted to a higher wavenumber (240 nm) and a new peak was appeared at 382 nm. This red-shifted could be attributed to modification and the increase in the electron density and structural reorganization in GO, due to its reduction in rMGO [21, 31].

Compared with the spectrum of rMGO, the 240 nm and 382 nm peaks shifted to 244 nm and 400 nm because of the high reduction of rMGO sheets and the SPR of Ag NPs. Furthermore, the peak at 400 nm was broad, and its intensity increased, and this could approve the loading of Ag NPs on rMGO.

The insets in Fig. 1A display dispersity of GO and rMGO-Ag nanocomposite in an aqueous solution with a concentration of 3 mg ml^{-1}, was sonicated for one h, and then preserved at room temperature for six weeks. After one week, sheets of GO sediment, while the rMGO-Ag nanocomposite was stable for more than six weeks. This high stability in the aqueous solution can be related to the repulsion of charged ions on nanocomposite and was confirmed with the z potential data.
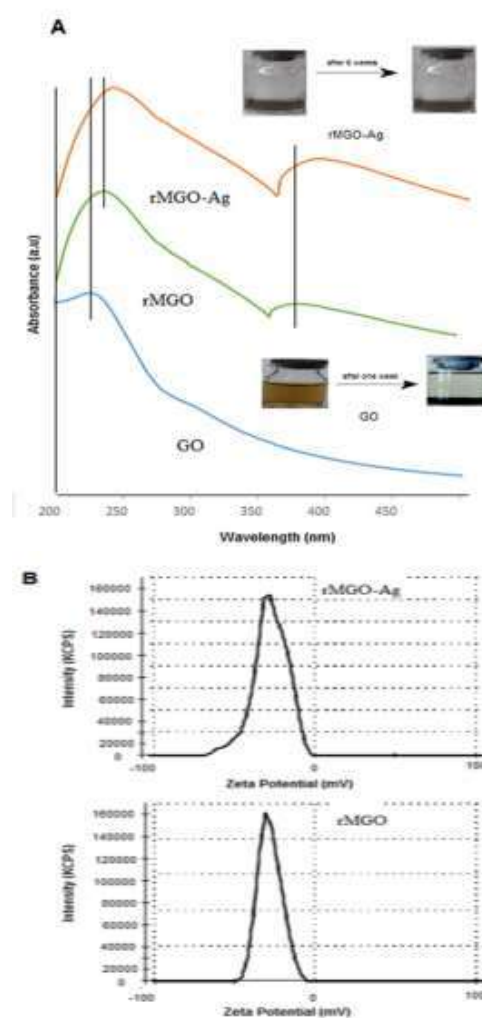
Fig. 1. UV-Vis spectra of A: GO, rMGO, and rMGO-Ag nanocomposite, Dispersions of GO rMGO-Ag nanocomposite (3mg ml^{-1}) in distilled water (inset), B: Zeta potential distribution of rMGO, and rMGO-Ag nanocomposite.

To measure the stability, and the surface charges on rMGO and rMGO-Ag, the Zeta potential of samples was studied in an aqueous medium with pH:12 (Fig. 1B). The average value of zeta potential in the surfaces of rMGO and rMGO-Ag is -29.4 mV and -34.8 mV, respectively. The negative charge on the rMGO is due to the presence of functional groups on the surface. The high negative charge of rMGO-Ag sheets shows the colloidal stability of nanocomposite in the aqueous media due to the electrostatic repulsive interactions between interlayer surface charges and the presence of Ag NPs. Comparison of colloidal stability Ag NPs in this work with Gly-Ag NPs (-23.1 mV) and rGO-Gly-Ag NPs (-32.5 mV) [21] shows high stability of this work and this could be attributed to the modification of GO with Gly and then synthesis of Ag NPs on modified GO.

Fig. 2 shows the XRD patterns of GO and rMGO-Ag nanocomposite. In XRD of GO, the sharp peek with an interlayer distance of about 0.82 nm at 10.8° attributes to the (001) diffraction peak of GO [13, 32, 33]. For rMGO-Ag nanocomposite, the diffraction peak (001) of GO was disappeared, and new peaks appeared. A peak at 2θ= 24.4 attribute to the (002) of reduced GO [13], and other new peaks at about 15.5, 19.1, 30.3, 34.3, and 36.2 correspond to the organized crystal structure of Gly [34]. Furthermore, in the XRD pattern of the nanocomposite, the diffraction peaks at 38.3 (111), 44.3 (200), 64.6 (220), and 77.6 (311) attributes to the planes of silver NPs [13, 32]. Based on Debye-Scherer's equation [33], the crystallite size of Ag is about 12.7 nm (FWHM=0.79°) that is proved with the TEM image.

Fig. 3 presents the FT-IR spectra of GO, rMGO, and rMGO-Ag nanocomposite. GO exhibits various bands at ν (cm^{-1}): 3408, 1727, 1621, 1228, and 1032 correspond to stretching vibration of the hydroxyl group, the carboxyl C=O, aromatic C=C, epoxy C–O and alkoxy C–O, respectively [13]. The presence of a peak at 1422 cm^{-1} attributed to the C-O peak of carboxy groups shows the highest oxidation of graphite to GO [35]. The presence of C=C groups displays that although graphite has been oxidized into GO, the main structure of layer graphite has still been retained. A comparison of the FT-IR spectra of GO and rMGO shows that the peaks due to carbonyl (1727 cm^{-1}) and epoxy (1228 cm^{-1}) of GO have entirely disappeared, the peak attributed to the alkoxy group (C–O) at 1032 cm^{-1} in GO also became relatively weak and broad [36]. On the other hand, in rMGO, the intensity of the C-O peak of carboxy groups decreased and shifted to 1380 cm^{-1}, and new peaks attributed to the CH$_2$ groups of Gly were appeared at 2932 and 2856 cm^{-1} [20]. These changes display the modification of GO with Gly and the complete reduction of modified graphite oxide (MGO) to rMGO using Gly as a reducing agent. In the FT-IR of the rMGO-Ag nanocomposite, the intensity of all peaks that attributed to the oxygenous groups decreased, which can be related to interaction rMGO sheets and Ag NPs [13].

Fig. 2. XRD patterns of GO, and rMGO-Ag nanocomposite.
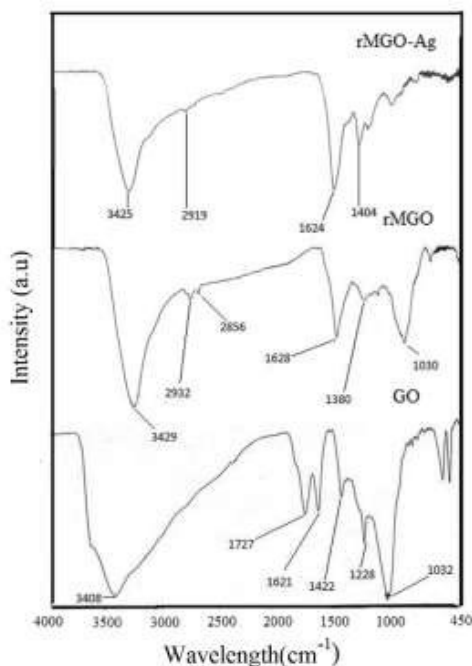
Fig. 3. FT-IR of GO, rMGO, and rMGO-Ag nanocomposite.

The formation of layered GO, modification of GO, and the loading of Ag on rMGO were confirmed by the FESEM and TEM studies. As shown in Fig. 4, the SEM image of GO is as layered nanosheets with folded edges. With the modification of GO, the crumpled structure is seen that can be attributed to the presence of modifiers and reduction process. The thin structure of the rMGO sheets and smooth surface with some corrugation propose a flexible structure of the rMGO sheets. Fig. 4 displays FE-SEM images of the rMGO-Ag nanocomposite at two magnifications. With the formation of silver particles on the surface of rMGO, the crumpled thin layers became more, and fine particles have appeared as the anemone flower on the surface.

To study the surface element contents and the presence of Ag on the surface of rMGO, the EDX technique can also be used (Figure 4, inset). The signals of elements confirmed the presence of N, C, and O on rMGO and also Ag on the surface of the rMGO-Ag.
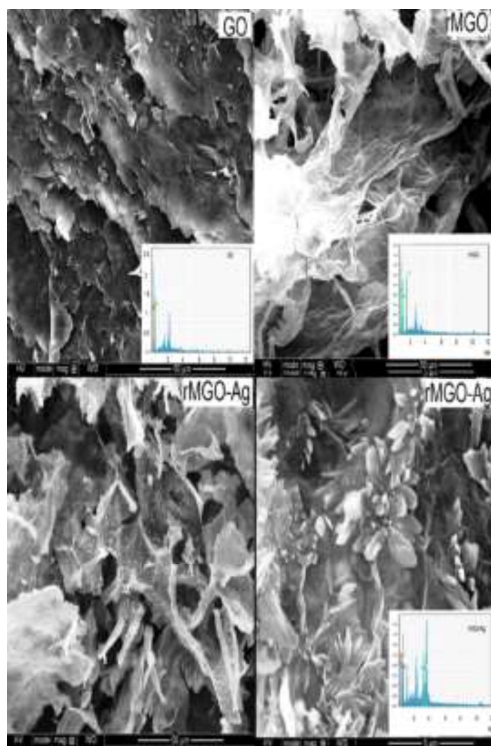
Fig.4 SEM-EDAX of GO, rMGO and rMGO-Ag nanocomposite.

The TEM images show the formation of spherical Ag nanoparticles on the crumbled surfaces of the rMGO sheets with an average particle size of 14 nm (Fig. 5). The FE-SEM and TEM images indicate the formation of spherical nanoparticles on crumpled layer rMGO.
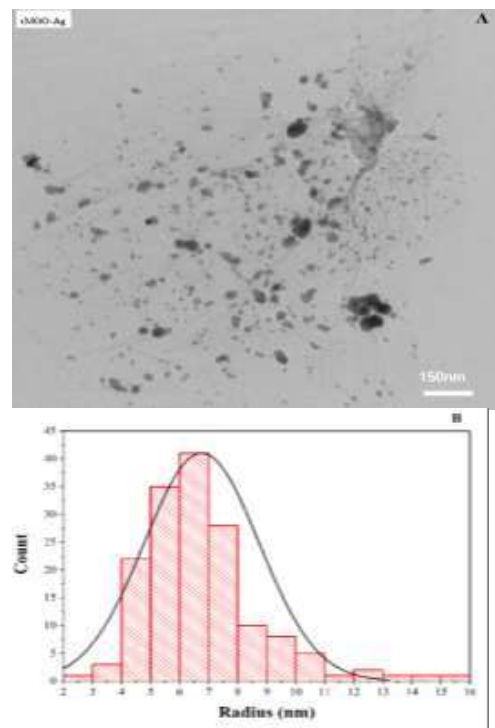
Fig. 5. A: TEM image of rMGO-Ag nanocomposite. B: The size distribution of Ag NPs in rMGO-Ag nanocomposite.

3.2. Reduction of 4-NP and 4-NA with rMGO-Ag nanocomposite

The catalytic activity of rMGO-Ag nanocomposite was studied for the reduction of 4-NP by $NaBH_4$. The aqueous solution of 4-NP displayed an absorption maximum at 320 nm due to the n - π* transitions that with the addition of $NaBH_4$, this peek shifted to 400 nm because of the producing of 4-nitrophenolate (Fig. 6A) [37]. Without a nanocatalyst, this peak stayed unchanged until 24 h. When the rMGO-Ag nanocomposite was added to the reaction mixture, compound's color became colorless; the peak height at 400 nm decreased and disappeared after 240 s (Fig. 6B).

All of these changes indicate the successful reduction of 4-NP. For 4-NP, Ln (A_t/A_0) decreased linearly with reaction time (Fig. 6C). Based on the pseudo-first-order reaction, the rate constant (k) was calculated by equation Ln (A_t/A_0) =-Kt via measuring the changes in absorbance of 4-NP (A_t) at 400 nm nm [38] (Fig. 6D). K, A_t, and A_0 are rate constant, initial absorbance, and absorbance at time t that, the rate constant was determined as 1.2×10^{-3} s^{-1} for 4-NP. The comparison of the catalytic behavior of rMGO-Ag nanocomposite for the reduction of 4-NP with previously reported catalysts was shown in Table 1.

Table 1. Comparison of the catalytic activity of rMGO-Ag nanocomposite for the reduction of 4-NP with other catalysts.

Catalyst	Dosage of catalyst (mg)	4-NP Concentration (mM)	NaBH4 Concentration (mM)	Reaction Time (min)	K (S^{-1})	k (S^{-1})	Ref.
rMGO-Ag nanocomposite	0.1	5×10^{-1} , 1ml	80 , 1ml	4	1.2×10^{-3}	12×10^{-3}	This work
Ag-carbon sphere	1	5×10 -5, 3 ml	100, 0.2	25	1.69×10^{-3}	1.69×10^{-3}	[44]
Ag-GO-poly(amidoamine) dendrimer nanocomposite	2.5	5, 1 ml	5	2	$21.7*10^{-3}$	8.68×10^{-3}	[45]
hollow silver nanospheres	0.1	5×10^{-1} , 1ml	80 , 1ml	6	$1.83*10^{-3}$	1.83×10^{-3}	[46]
L-Arginine – Ag-rGO nanocomposites	1	2×10^{-1}, 20 ml	100, 5 ml	12	6.91×10^{-3}	6.91×10^{-3}	[11]
LrGO-Ag20Au80	12	9.6×10^{-5}	0.1	1.7	11×10^{-3}	0.92×10^{-3}	[47]

k: K/ Dosage of catalyst
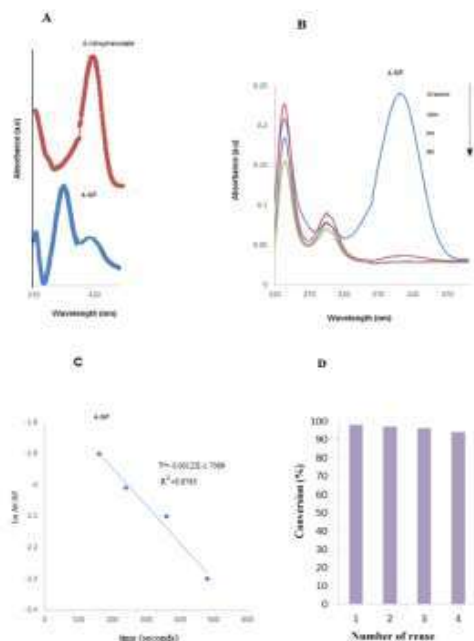
Fig. 6. Successive UV–Vis absorption spectra of A: 4-NP and 4-nitrophenolat, B: the reduction of 4-NP by NaBH₄ in the presence of rMGO-Ag nanocomposite and C: Plot of ln A$_t$/A$_0$ versus time for the reduction of 4-NP using rMGO-Ag, D: Reusability of rMGO-Ag nanocomposite towards 4-NP reduction.

The results displayed that rMGO-Ag nanocomposite with low dosage is more active that this could be related to Ag NPs or modified reduced graphene oxide surface. The recycling of the nanocatalyst was studied and displayed in Fig. 6B (inset). After each reaction, the nanocomposite was recycled and reused four times with high efficiency. Low activity of nanocomposite after the fourth run may be due to the aggregation of Ag NPs or saturation surface of rMGO. In the reduction process, 4-nitrophenolate anions are adsorbed onto the rMGO-Ag nanocatalyst, and then the electron released from BH4- reduces the 4-nitrophenolate ion to 4-aminophenol. [39]. The electron transfer process depends on the available surface area of the catalyst and the number of nanoparticles on the surface [39, 40], with increasing the number of nanoparticles and the surface area of the nanocatalyst, the reaction rate increases.

3.3. Antibacterial activity of resultant nanocomposite
The MIC of the rMGO-Ag nanocomposite, GO, and rMGO was investigated by the Broth-dilution method. The results displayed that GO and rMGO have no inhibition in bacterial growth. Based on preview researches, some of GO sheets showed no antibacterial activity, and some of them showed high antibacterial activity because of the sharp edges and the oxidant nature of GO sheets [13, 41]. Fig. 7 displays the bacteria growth on agar plates at different concentrations of rGO/MAg nanocomposite against E-coli and S-arouses.
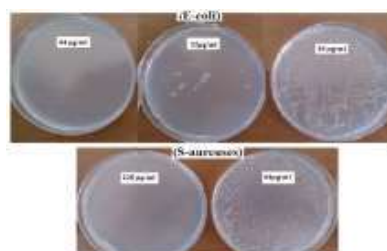
Fig. 7. The bacteria growth on agar plates at different concentrations of of rMGO-Ag nanocomposite against E-Coli (upper) and S-aureuses (bottom).

The MIC values of rMGO-Ag nanocomposite against E-coli and S-arouses are 32μg/ml, and 64μg/ml, respectively. The antibacterial activity of resultant nanocomposite is higher than it for our previous researches [13]. The size, shape, environment of silver nanoparticles, and the difference in the structure of the bacterial wall have displayed significant impacts on their antibacterial activity [42, 43]. The antibacterial effect of rMGO-Ag nanocomposite could be described according to this method: Ag NPs, sharp edges of rMGO, or both can attach to the cell surface, penetrate inside bacteria and disturb them [41, 42].

3.4. Electrochemical determination of H_2O_2

The cyclic voltammogram of the bare PGE in HCl 0.1 M was recorded, and the obtained voltammogram is presented as the dotted line in Fig. 9. As expected, no obvious redox peak can be observed on the PGE in the studied potential range. However, at the PGE modified with rMGO-Ag nanocomposite, a reversible redox peak can be observed indicating the successful immobilization of rMGO-Ag nanocomposite on the electrode surface (Fig. 8 dashed line). In the presence of 1 mM H_2O_2, there was a dramatic enhancement of cathodic peak current due to intense electrocatalytic activity of rMGO-Ag nanocomposite for electroreduction of H_2O_2 (Fig. 8, the solid line). The cathodic peak potential of reduction of H_2O_2 at rMGO-Ag-PGE was about -0.3 V. On the other hand, on the bare PGE, the very weak peak was observed at the more negative potential in the presence of the same amount of H_2O_2. Consequently, compared with PGE, on the rMGO-Ag-PGE signicant reduction of overpotential and dramatic increase of peak current was achieved in the presence of H_2O_2.
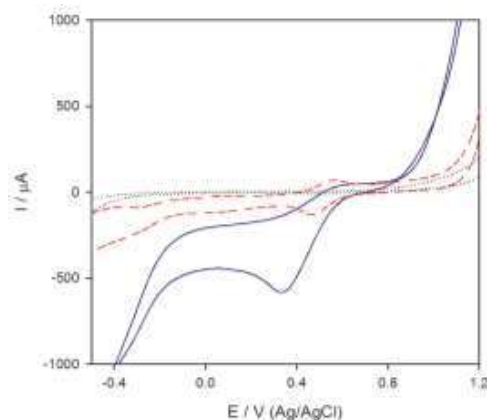
Fig. 8. Cyclic voltammograms obtained in HCl 0.1 M at 50 mVs⁻¹ on the (dotted line) bare PGE and (dashed line) rMGO-Ag-PGE. The solid line was the cyclic voltammograms obtained in HCl 0.1 M containing 1 mM H_2O_2 at 50 mVs⁻¹ on the

Fig. 9 shows the influence of the concentration of H_2O_2 on the cyclic voltammograms of the rMGO-Ag-PGE. Upon the successive addition of H_2O_2 (10-1000 μM), the cathodic peak current were increased accordingly. The CV peak currents showed a linear correlation to H_2O_2 concentrations in the range from 10 to 1000 μM H_2O_2. Detection limit of H_2O_2 was estimated from the calibration equation as 9.4 μM (based on S/N=3). From the slope of the calibration curve, the concentration sensitivity was obtained as 0.52 μA μM⁻¹.
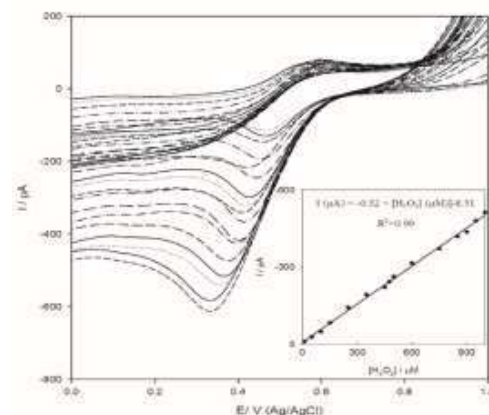
Fig. 9. Cyclic voltammograms obtained at 50 mVs⁻¹ on the rMGO-Ag-PGE in HCl 0.1 M containing 10-1000 μM H_2O_2. Inset shows the calibration carve obtained from the reduction electrocatalytic peaks currents.

4. CONCLUSION

A green method was used for in situ nucleation, and growth of AgNPs on rMGO using Glycine-modified GO as reducing as well as a stabilizing agent of Ag NPs. Modification and reduction of exfoliated GO (rMGO) sheets were carried out in an aqueous medium by glycine amino acid, and then rMGO acted as reducing and stabilizer agent of $AgNO_3$ at 80 °C. The chemical structure of the resultant suspension nanocomposite was analyzed after the freeze-drying by UV-Vis, XRD, FT-IR, FE-SEM, EDAX, and TEM. Zeta potential data showed that, the modification of GO with Gly, improve the stability of Ag NPs rather than Gly modified Ag–GO. Therefore, this obtained nanocomposite is a biocompatible component and method is an eco-friendly synthesis to layer graphene sheets, and in situ AgNPs decorated rMGO. Finally, the resultant nanocomposite showed high catalytic and electrocatalytic activity towards the reduction of 4-NP and H_2O_2, and also excellent antibacterial behavior against E-coli and S-arouses.

REFERENCES

[1] E. Abbasi. M. Milani. S. Fekri Aval. M. Kouhi. A. Akbarzadeh. H. Tayefi Nasrabadi.

P. Nikasa. S.W. Joo, Y. Hanifehpour and K. Nejati-Koshki. Silver nanoparticles: synthesis methods, bio-applications and properties. *Crit. Rev. Microbiol.* 42 (2016) 173-180.

[2] J.M. Baik. S.J. Lee and M. Moskovits. Polarized surface-enhanced Raman spectroscopy from molecules adsorbed in nano-gaps produced by electromigration in silver nanowires. *Nano. Lett.* 9 (2009) 672-676.

[3] Y. Junejo. A. Baykal. M. Safdar and A. Balouch. A novel green synthesis and characterization of Ag NPs with its ultra-rapid catalytic reduction of methyl green dye. *Appl. Surf. Sci.* 290 (2014) 499-503.

[4] Y. Wang. L. Chen and P. Liu. Biocompatible Triplex Ag@ SiO2@ mTiO2 Core–Shell Nanoparticles for Simultaneous Fluorescence-SERS Bimodal Imaging and Drug Delivery. *Chem. Eur. J.* 18 (2012) 5935-5943.

[5] J. García-Barrasa. J.M. López-de-Luzuriaga and M. Monge. Silver nanoparticles: synthesis through chemical methods in solution and biomedical applications. Cent. Eur. J. Chem. 9 (2011) 7- . 19.

[6] H. Erjaee. H. Rajaian and S. Nazifi. Synthesis and characterization of novel silver nanoparticles using Chamaemelum nobile extract for antibacterial application.Adv. Nat. Sci.: Nanosci. Nanotechnol.

[7] Z. Sui. X. Chen. L. Wang. L. Xu. W. Zhuang. Y. Chai and C. Yang, Capping effect of CTAB on positively charged Ag nanoparticles. Phys. E: Low-Dimens. Syst. Nanostructures. 33 (2006) 308-314.

[8] C. Singh. M.A. Ali and G. Sumana. Green synthesis of graphene based biomaterial using fenugreek seeds for lipid detection ACS. Sustain. Chem. Eng. 4 (2016) 871-880.

[9] J.T. Robinson. F.K. Perkins, E.S. Snow. Z. Wei and P.E. Sheehan. Reduced graphene oxide molecular sensors. Nano. Lett. 8 (2008) 3137-3140.

[10] S. Gilje. S. Han, M. Wang. K.L. Wang and R.B. Kaner. A chemical route to graphene for device applications. Nano. Lett. 7 (2007) 3394-3398.

[11] T.K. Das. P. Bhawal. S. Ganguly, S. Mondal and N.C. Das. A facile green synthesis of amino acid boosted Ag decorated reduced graphene oxide nanocomposites and its catalytic activity towards 4-nitrophenol reduction. *Surf. Interfaces.* 13 (2018) 79-91.

[12] B. Yang. Z. Liu. Z. Guo. W. Zhang. M. Wan. X. Qin and H. Zhong. In situ green synthesis of silver–graphene oxide nanocomposites by

using tryptophan as a reducing and stabilizing agent and their application in SERS. *Appl. Surf. Sci.*316 (2014) 22-27.

[13] S. Fathalipour. S. Pourbeyram. A. Sharafian. A. Tanomand and P. Azam. synthesis of Ag/reduced graphene oxide nanocomposite with excellent electrocatalytic and antibacterial performance. *Mater. Sci. Eng. C*. 75 (2017) 742-751.

[14] J. Shen. M. Shi. B. Yan. H. Ma. N. Li and M. Ye. One-pot hydrothermal synthesis of Ag-reduced graphene oxide composite with ionic liquid. *J. Mater. Chem.* 21 (2011) 7795-7801.

[15] K. Ojha. O. Anjaneyulu and A.K. Ganguli. Graphene-based hybrid materials: synthetic approaches and properties. *Curr. Sci.* 107 (2014) 397-418.

[16] O. Akhavan. E. Ghaderi. S. Aghayee. Y. Fereydooni and A. Talebi. The use of a glucose-reduced graphene oxide suspension for photothermal cancer therapy. *J. Mater. Chem.* 22 (2012) 13773-13781.

[17] J. Gao. F. Liu. Y. Liu. N. Ma.Z. Wang and X. Zhang. Environment-friendly method to produce graphene that employs vitamin C and amino acid. *Chem. Mater.* 22 (2010) 2213-2218.

[18] Y. Feng. N. Feng and G. Du. A green reduction of graphene oxide via starch-based materials. *RSC Adv.*,3 (2013) 21466-21474.

[19] D.R. Dreyer. S. Park. C.W. Bielawski and R.S. Ruoff, The chemistry of graphene oxide. Chemical society reviews. *Chem. Soc. Rev.* 39 (2010) 228-240.

[20] S. Bose. T. Kuila. A.K. Mishra. N.H. Kim and J.H. Lee. Dual role of glycine as a chemical functionalizer and a reducing agent in the preparation of graphene: an environmentally friendly method. *J. Mater. Chem. A*. 22 (2012) 9696-9703.

[21] S. Fathalipour and E. Abdi. Glycine-assisted aqueous suspension of reduced graphene oxide/Ag nanocomposite via in situ reduction at room temperature: synthesis and electroactivity behavior. *Synth. Met.* 221 (2016) 159-168.

[22] K. Hamaguchi. H. Kawasaki and R. Arakawa. Photochemical synthesis of glycine-stabilized gold nanoparticles and its heavy-metal-induced aggregation behavior. olloids Surf. A Physicochem. *Eng. Asp.*367 (2010) 167-173.

[23] P. Guo L. Tang J. Tang. G. Zeng, B. Huang. H. Dong. Y. Zhang.Y. Zhou. Y. Deng and L. Ma. Catalytic reduction–adsorption for removal of p-nitrophenol and its conversion

p-aminophenol from water by gold nanoparticles supported on oxidized mesoporous carbon. *J. Colloid Interface Sci.* 469 (2016) 78-85.

[24] M.I. Din. R. Khalid. Z. Hussain. T. Hussain, A. Mujahid. J. Najeeb and F. Izhar. Nanocatalytic Assemblies for Catalytic Reduction of Nitrophenols: *Crit. Rev. Anal. Chem.* 50 (2020) 322-338.

[25] M. Singla. A. Negi, V. Mahajan.K. Singh and D. Jain. Catalytic behavior of nickel nanoparticles stabilized by lower alkylammonium bromide in aqueous medium. *Appl. Catal. A.* 323 (2007) 51-57.

[26] N. Li. P. Zhao and D. Astruc. Anisotropic gold nanoparticles: synthesis, properties, applications, and toxicity. *Angew. Chem. Int. Ed,* 53 (2014) 1756-1789.

[27] N. Meng. S. Zhang.Y. Zhou. W. Nie and P. Chen. Novel synthesis of silver/reduced graphene oxide nanocomposite and its high catalytic activity towards hydrogenation of 4-nitrophenol. *RSC* Adv.5 (2015) 70968-70971.

[28] T. Aditya. A. Pal and T. Pal. Nitroarene reduction: a trusted model reaction to test nanoparticle catalysts. *Chem. Commun.* 51 (2015) 9410-9431.

[29] T. Wu. L. Zhang. J. Gao. Y. Liu.C. Gao and J. Yan. Fabrication of graphene oxide decorated with Au–Ag alloy nanoparticles and its superior catalytic performance for the reduction of 4-nitrophenol. *J. Mater. Chem. A*. 1 (2013) 7384-7390.

[30] D.C. Marcano. D.V. Kosynkin. J.M. Berlin. A. Sinitskii. Z. Sun. A. Slesarev. L.B. Alemany.W. Lu and J.M. Tour. Improved synthesis of graphene oxide. *ACS .nano.* 4 (2010) 4806-4814.

[31] A.B. Bourlinos. D. Gournis. D. Petridis. T. Szabó. A. Szeri and I. Dékány. Graphite oxide: chemical reduction to graphite and surface modification with primary aliphatic amines and amino acids. *Langmuir.* 19 (2003) 6050-6055.

[32] S. Pourbeyram. M. Soltanpour. S. Fathalipour, Determination of Phosphate in Human Serum with Zirconium/Reduced Graphene Oxide Modified Electrode. 35 (2019)739-743.

[33] S. Fathalipour. B. Ataei and F. Janati. Aqueous suspension of biocompatible reduced graphene oxide-Au NPs composite as an effective recyclable catalyst in a Betti reaction. *Mater. Sci. Eng. C*.97 (2019) 356-366.

[34] X. Yang. C.B. Ching. X.J. Wang. J. Lu., AICHE annual meeting, San Fransisco, *CA,* 2006.

[35] B. Zahed and H. Hosseini-Monfared. A comparative study of silver-graphene oxide nanocomposites as a recyclable catalyst for the aerobic oxidation of benzyl alcohol: Support effect. *Appl. Surf. Sci.* 328 (2015) 536-547.

[36] A. Kumar and M. Khandelwal. Amino acid mediated functionalization and reduction of graphene oxide–synthesis and the formation mechanism of nitrogen-doped graphene. *New J. Chem.*38 (2014) 3457-3467.

[37] S. Yang. C. Nie. H. Liu and H. Liu. Facile synthesis and catalytic application of Ag–Fe2O3–carbons nanocomposites. *Mater. Lett.* 100 (2013) 296-298.

[38] N. Pradhan. A. Pal and T. Pal. Catalytic reduction of aromatic nitro compounds by coinage metal nanoparticles. *Langmuir.* 17 (2001) 1800-1802.

[39] P. Veerakumar. M. Velayudham. K.-L. Lu and S. Rajagopal. Polyelectrolyte encapsulated gold nanoparticles as efficient active catalyst for reduction of nitro compounds by kinetic method. *Appl. Catal. A: Gen.* 439 (2012) 197-205.

[40] N.C. Sharma. S.V. Sahi. S. Nath. J.G. Parsons. J.L. Gardea-Torresde and T. Pal. Synthesis of plant-mediated gold nanoparticles and catalytic role of biomatrix-embedded nanomaterials. *Environ.sci. technol.* 41 (2007) 5137-5142.

[41] M. Zhang. Y. Zhao. L. Yan. R. Peltier. W. Hui. X. Yao.Y. Cui. X. Chen. H. Sun and Z. Wang. Interfacial engineering of bimetallic Ag/Pt nanoparticles on reduced graphene oxide matrix for enhanced antimicrobial activity. *ACS Appl. Mater. Interfaces.* 8 (2016) 8834-8840.

[42] V.K. Sharma. R.A. Yngard and Y. Lin. Silver nanoparticles: green synthesis and their antimicrobial activities. *Ad.colloid. interfac.* 145 (2009) 83-96.

[43] L. Kvítek. A. Panáček. J. Soukupova. M. Kolář. R. Večeřová. R. Prucek. M. Holecova and R. Zbořil. Effect of surfactants and polymers on stability and antibacterial activity of silver nanoparticles (NPs). *J. Phys. Chem. C*. 112 (2008) 5825-5834.

[44] S. Tang.S. Vongehr and X. Meng. Carbon spheres with controllable silver nanoparticle doping. *J. Phys. Chem. C*. 114 (2009) 977-982.

[45] R. Rajesh and R. Venkatesan. Encapsulation of silver nanoparticles into graphite grafted with hyperbranched poly (amidoamine) dendrimer and their catalytic activity towards reduction of nitro aromatics. *J. Mol. Catal. A. Chem.* 359 (2012) 88-96.

[46] R. Vadakkekara. M. Chakraborty and P.A. Parikh. Reduction of aromatic nitro compounds on colloidal hollow silver nanospheres. *Colloids Surf. A Physicochem. Eng. Asp.* 399 (2012) 11-17.

[47] Z. Çıplak. B. Getiren. C. Gökalp. A. Yıldız and N. Yıldız. Green synthesis of reduced graphene oxide-AgAu bimetallic nanocomposite: *Catalytic performance. Chem. Eng. Commun.* (2019) 1-15.

نانوذرات نقره در بستر گرافن اکسید اصلاح شده با گلیسین برای کاربردهای کاتالیزوری، الکتروکاتالیزوری و ضد میکروبی

سهراب فتحعلی پور¹، سیما پور بیرام¹**، ساناز لطفی¹، رسول بولگار²

۱. گروه شیمی، دانشکده علوم پایه، دانشگاه پیام نور، تهران، ایران

۲. دانشکده علوم، دانشگاه شهید مدنی، آذربایجان، ایران

نانوکامپوزیت نقره-اکسید گرافن کاهش یافته، از طریق هسته زایی درجای نانوذرات نقره درسطح گرافن اکسید کاهش یافته و اصلاح شده تهیه شد. گلیسین به عنوان کاهنده سبز و همچنین عامل اصلاح کننده‌ی گرافن اکسید در تهیه‌ی نانوکامپوزیت استفاده شد. هسته شدن نانودرات نقره در دمای ۸۰ درجه سانتیگراد در محیط های آبی انجام می شود. کاهش، اصلاح و سنتز نانو ذرات توسط تکنیک های UV-Vis، FT-IR و XRD تأیید شد. در همین حال، مورفولوژی نانوکامپوزیت با تصاویر SEM و TEM مورد مطالعه قرار گرفت. نانوکامپوزیت سنتز شده در کاهش ۴-نیتروفنول توسط سدیم بوروهیدرید رفتار کاتالیزوری عالی نشان داد. رفتار الکتروکاتالیستی الکترود مغز مداد اصلاح شده با نانوکامپوزیت برای کاهش الکتریکی هیدروژن پراکسید توسط ولتامتری چرخه ای بررسی شد. در شرایط مطلوب هیدروژن پراکسید با حد تشخیص ۹٫۴ میکرومولار و حساسیت ۰٫۵۲ میکروآمپر بر میکرو مولار تعیین شد. علاوه بر این، با بررسی داده های MIC نانوکامپوزیت، مشخص شد که این ترکیب دارای فعالیت ضد باکتری عالی است.

واژه‌های کلیدی

گرافن اکسید؛ نانوذرات نقره؛ سنتز سبز؛ الکتروکاتالیزوری؛ ضد میکروبی.